

This is an Open Access document downloaded from ORCA, Cardiff University's institutional repository: <https://orca.cardiff.ac.uk/id/eprint/103404/>

This is the author's version of a work that was submitted to / accepted for publication.

Citation for final published version:

D'Agostino, Carmine, Brett, Gemma Louise, Divitini, Giorgio, Ducati, Caterina, Hutchings, Graham John, Mantle, Michael D. and Gladden, Lynn F. 2017. Increased affinity of small gold particles for glycerol oxidation over Au/TiO<sub>2</sub> probed by NMR relaxation methods. *ACS Catalysis* 7 (7), pp. 4235-4241. 10.1021/acscatal.7b01255

Publishers page: <http://dx.doi.org/10.1021/acscatal.7b01255>

Please note:

Changes made as a result of publishing processes such as copy-editing, formatting and page numbers may not be reflected in this version. For the definitive version of this publication, please refer to the published source. You are advised to consult the publisher's version if you wish to cite this paper.

This version is being made available in accordance with publisher policies. See <http://orca.cf.ac.uk/policies.html> for usage policies. Copyright and moral rights for publications made available in ORCA are retained by the copyright holders.



# Increased Affinity of Small Gold Particles for Glycerol Oxidation over Au/TiO<sub>2</sub> Probed by NMR Relaxation Methods

Carmine D'Agostino,<sup>\*,†</sup> Gemma Brett,<sup>‡</sup> 16,17 Giorgio Divitini,<sup>§</sup> Caterina Ducati,<sup>§</sup> Graham J. Hutchings,<sup>‡</sup> Michael D. Mantle,<sup>†</sup> and Lynn F. Gladden<sup>†</sup>

<sup>†</sup>Department of Chemical Engineering and Biotechnology, University of Cambridge, Pembroke Street, Cambridge CB2 3RA, United Kingdom

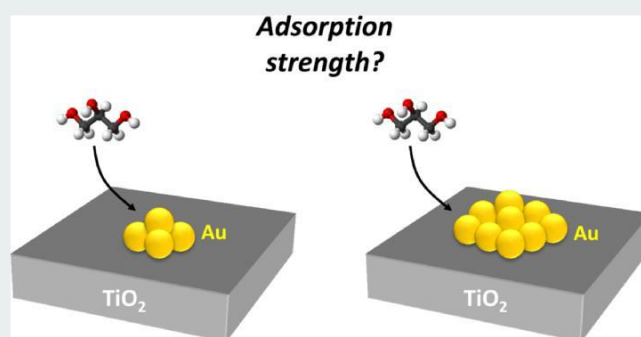
<sup>29,30</sup> <sup>‡</sup>Cardiff Catalysis Institute, Cardiff University, Cardiff CF10 3AT, United Kingdom

<sup>§</sup>Department of Material Science and Metallurgy, University of Cambridge, 27 Charles Babbage Road, Cambridge CB3 0FS, United Kingdom

**ABSTRACT:** The aerobic oxidation of glycerol in aqueous solution over Au/TiO<sub>2</sub> catalysts has been studied, and the effect of Au loading by wet impregnation, in the range 0.5–5% Au, has been assessed. Low metal loading favors the deposition of smaller particles, whereas higher loadings lead to the formation of much larger gold particles, as revealed by scanning transmission electron microscopy (STEM) analysis. Reaction studies show that a higher metal loading has a detrimental effect on the catalyst activity, which decreases significantly as the Au load increases. In addition to reaction studies, <sup>1</sup>H NMR T<sub>1</sub>/T<sub>2</sub> relaxation time<sup>16,17</sup> measurements have been used to assess the effect of metal loading and particle size

on the adsorption properties of glycerol (reactant) and water (solvent) within the catalyst. The NMR results show that the adsorption properties of glycerol relative to water as a function of the Au loading have a similar trend to that observed for the reactivity, with glycerol exhibiting a higher surface affinity relative to water for the catalyst with low Au loading. The overall results indicate that metal loading significantly affects the typical Au particle size, which, in turn, affects both the reaction and adsorption properties of glycerol over the catalyst surface. In particular, the trend in T<sub>1</sub>/T<sub>2</sub> ratio clearly indicates that glycerol has a much stronger affinity with smaller gold particles, which is an important factor in promoting glycerol oxidation. This result is of great significance in understanding the reactivity of polyols over supported gold catalysts and gives the first experimental evidence that smaller gold particles tend to be stronger adsorption sites for glycerol, in agreement with computational and theoretical studies.

**KEYWORDS:** glycerol oxidation, gold catalysis, metal loading, NMR relaxometry, STEM



## INTRODUCTION

In recent years, the oxidation of renewable feedstocks has become a topic of general interest in view of a more green or sustainable production of value-added chemicals.<sup>1–4</sup> In particular, glycerol is often considered as a “platform” chemical,<sup>3–7</sup> as it is a highly functionalized molecule and is widely available, being the main byproduct of the biodiesel production process.<sup>8,9</sup> The oxidation of glycerol results in a large number of fine chemicals, such as dihydroxyacetone, glyceric acid, and tartronic acid, to mention some.<sup>4,5,10,11</sup> The use of dioxygen is undoubtedly the greener way to carry out such reactions, and current interest lies in the use of heterogeneous catalysts, due to their advantages in terms of catalyst reusability, separation, and stability. Although the commercialization of such processes is still at an early stage, several studies on glycerol oxidation are now available in the scientific literature.<sup>3–5,10–14</sup> Due to the high viscosity, liquid-phase heterogeneously catalyzed oxidations of glycerol and

other polyols are usually carried out in the presence of a solvent; water is the solvent of choice,<sup>11,15–19</sup> as it is largely available and nontoxic. Several types of catalysts have been used for such reactions, and a particular focus in the past decade has been directed toward gold nanoparticles supported on mesoporous solids. Hutchings and Haruta were pioneers in discovering that gold nanoparticles supported on metal oxides are effective oxidation catalysts at relatively mild conditions,<sup>20</sup> and the use of this type of catalysts is currently attracting the attention of the scientific community for the liquid-phase oxidation of alcohols and polyols in general. Catalysts such as gold supported on porous TiO<sub>2</sub>, Al<sub>2</sub>O<sub>3</sub>, and activated carbon,<sup>10,13–15,21–23</sup> including gold alloyed with other metals, have been used for the oxidation of polyols.

<sup>1,11,24,25</sup>

Glycerol can be effectively oxidized to produce glycerate and mesoxalate on Au/TiO<sub>2</sub> prepared by the deposition-precipitation method.<sup>4</sup> The reaction is usually carried out in alkaline conditions, as this tends to avoid metal leaching and facilitates product desorption.<sup>26</sup> In recent developments, it has been reported that glycerol oxidation can be effectively carried out also in base-free conditions.<sup>12,27,28</sup> More recently, the effect of solvent composition on the catalytic activity of Au/TiO<sub>2</sub>

used in the oxidation of polyols has been reported, combining catalyst screening tests with NMR relaxation time measurements. This novel protocol allows the characterization of surface interaction strength in porous catalysts by measuring the spin-lattice, T<sub>1</sub>, and transverse spin, T<sub>2</sub>, relaxation time

constants and has been previously used to understand wettability and hydration in rocks, plasters, and concrete.<sup>31-33</sup> It has been suggested that the T<sub>1</sub>/T<sub>2</sub> ratio can be seen as analogous to an energy of adsorption over a surface;<sup>34</sup> this has recently been experimentally validated by combining NMR relaxation with temperature-programmed desorption (TPD) measurements.<sup>35</sup> It was shown that the T<sub>1</sub>/T<sub>2</sub> is particularly sensitive to the strength of the adsorption sites over the surface. The NMR relaxation methods offer several advantages, as such experiments are noninvasive, chemically selective, and with relatively short data acquisition times compared to many other methods and are particularly suitable to study liquids in porous materials.<sup>35</sup>

Recent studies on polyol oxidations over Au/TiO<sub>2</sub> suggest a strong dependence of catalyst activity upon the adsorption

strength of the reactant. Adsorption properties of different polyols were seen to vary greatly by changing the solvent composition and the type of polyols,<sup>17</sup> which indicated that the molecular structure of the polyols can greatly affect their adsorption over the catalyst surface. A major point of discussion in gold catalysis, particularly for glycerol oxidation reactions, is the effect of gold particle size on catalyst activity. The effect of gold loading on catalytic activity can be related to the particle size, and it has been reported that a lower metal loading leads to the deposition of smaller gold particles over the surface,<sup>36</sup> which has been reported to improve catalytic activity in glycerol oxidation reactions.<sup>24,37</sup> Dimitratos et al.<sup>24</sup> studied the effect of Au particle size in the liquid-phase oxidation of glycerol over Au/C catalysts and observed a decrease in catalyst activity with increasing particle size. Theoretical and computational studies have suggested that smaller Au particles favor the formation of stronger bonds with adsorbates such as glycerol.<sup>38,39</sup> However, such conclusions are still based on theoretical results, and according to our knowledge, there is as yet no clear understanding of how these smaller gold particles promote higher activity.

The purpose of this paper is to use NMR relaxation techniques to understand adsorption properties of glycerol as a function of metal loading, the latter reported to affect metal particle size, and understand what are the key factors explaining how smaller gold particles promote higher activity in glycerol oxidation. Early applications of NMR relaxation measurements to solid catalysts have shown the potential of the technique as a characterization tool to probe molecular adsorption, which can be used in combination with other methods in order to optimize catalyst selection and design.<sup>40</sup> In the current work, we have studied the oxidation of glycerol in aqueous solution over Au/TiO<sub>2</sub> catalysts, focusing on the effect of the Au content and particle size on the catalytic activity and on NMR relaxation times, in order to understand the dependence of

reaction and adsorption properties on the Au loading and particle size. We have also carried out scanning transmission electron microscopy (STEM) of the different Au/TiO<sub>2</sub> catalysts, in order to understand the relationship between surface morphology and NMR relaxation times. The results are of significance because: (i) they give fundamental insights into surface interactions of glycerol and water with Au supported catalysts; (ii) it is experimentally shown for the first time that smaller Au particles contribute to a stronger adsorption strength for glycerol relative to water over the catalyst surface, which may have significant implications in understanding the role of metal as well as support in heterogeneous catalysis.

## EXPERIMENTAL SECTION

**Materials and Methods.** Au/TiO<sub>2</sub> catalysts with different Au contents were prepared by wet impregnation of TiO<sub>2</sub> (Degussa, P25), using aqueous solutions of HAuCl<sub>4</sub>·3H<sub>2</sub>O (Johnson Matthey). The paste formed was ground and dried at 110 °C for 16 h and then calcined in static air, typically at 400 °C for 3 h. The 0%Au/TiO<sub>2</sub> solid sample was obtained using the same procedure but without contacting the solid TiO<sub>2</sub> with the gold precursor. Glycerol (≥99%) was obtained from Sigma-Aldrich. Deionized water was obtained by using a laboratory purification system (PURELAB option, Elga).

**Catalytic Experiments.** Catalytic reactions were carried out using a 50 mL Parr autoclave. The aqueous glycerol solution (0.6 M and NaOH/glycerol ratio = 2, mol/mol) was added into the reactor, and the desired amount of catalyst (glycerol/metal ratio = 500/2000, mol/mol) was suspended in the solution. The autoclave was pressurized with oxygen (10 bar pressure) and heated at 60 °C. The reaction mixture was stirred at 1500 rpm for 4 h. The reactor vessel was cooled to room temperature, and the reaction mixture was analyzed by HPLC with ultraviolet and refractive index detectors. Reactants and products were separated using a Metacarb 67H column. The eluent was an aqueous solution of H<sub>3</sub>PO<sub>4</sub> (0.01 M), and the flow was 0.45 mL min<sup>-1</sup>. Samples of the reaction mixture (0.5 mL) were diluted (to 5 mL) using the eluent. Products were identified by comparison with authentic samples. For the quantification of the amounts of reactants consumed and products generated, an external calibration method was used.

**NMR Experiments.** NMR experiments were performed in a Bruker Biospin DMX 300 operating at a <sup>1</sup>H frequency of 300.13 MHz. NMR relaxation experiments were performed using a T<sub>1</sub>-T<sub>2</sub> pulse sequence, which comprises a saturation recovery measurement to encode T<sub>1</sub> (using a comb of 90° pulses) followed by a Carr-Purcell Meiboom-Gill (CPMG) echo train of 180° pulses to encode T<sub>2</sub>. The sequence is schematically shown in Figure 1. The T<sub>1</sub> recovery interval, t<sub>delay</sub>, was varied logarithmically between 1 ms and 15 s in 32 steps. The echo spacing between the 180° pulses of the CPMG was set to 250 μs. More details of the pulse sequence used are reported elsewhere.<sup>35</sup> All NMR measurements were carried out at room temperature.

**STEM Characterization.** The samples, in dry powder form, were dispersed on standard Cu grids for transmission electron microscopy. A FEI Tecnai F20 S/TEM with an acceleration voltage of 200 kV was used; acquisition was carried out in scanning mode (STEM) using the high-angle annular dark field (HAADF) signal. Image processing and analysis were carried out with ImageJ.



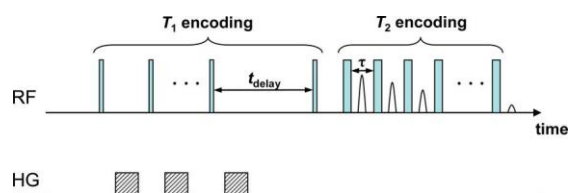


Figure 1.  $T_1$ - $T_2$  NMR pulse sequence. The thin and thick vertical bars represent  $90^\circ$  and  $180^\circ$  radiofrequency (RF) pulses, respectively.  $T_1$  relaxation is encoded in the variable time  $t_{\text{delay}}$ .  $T_2$  relaxation is encoded in the train of  $n$   $180^\circ$  pulses. A single data point is acquired at the center of each echo time,  $\tau$ . The application of homospoil magnetic field gradients (HG) is identified by the cross-hatched patterns.

## RESULTS AND DISCUSSION

**Glycerol Oxidation and Competitive Adsorption.** The conversion for the glycerol oxidation (at 4 h final reaction time) is reported in Figure 2 as a function of Au mean particle size,

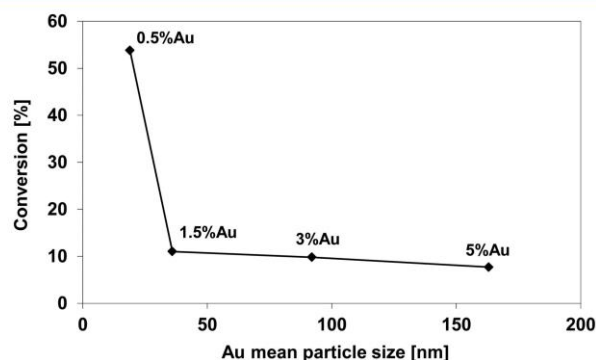


Figure 2. Conversion at 4 h time for glycerol oxidation on Au/TiO<sub>2</sub> catalyst as a function of Au mean particle size. Indication of the corresponding Au loading is also reported. The solid line is a guide to the eye.

which is related to the Au loading, also reported in the same figure. The 0.5% Au/TiO<sub>2</sub>, which is the catalyst with the smallest Au particle size, shows the highest conversion, with a value of 54%. The conversion decreases significantly to 11% for the 1.5% Au/TiO<sub>2</sub> and continues a steady decrease down to approximately 7% for the 5% Au/TiO<sub>2</sub>, along with an increase in Au particle size. The main reaction products were in all cases glycolic acid (~40%), formic acid (~30%), and glyceric acid (~30%), with very small amounts of oxalic acid detected.

Given that the catalysts are all prepared with the same method using the same precursors, it seems reasonable to assume that the dramatic drop in conversion as a function of metal load has to be associated with structure sensitivity processes over the catalyst surface.

In order to understand the origin of catalyst activity, we have used NMR relaxation time measurements to probe the  $T_1$  and  $T_2$  relaxation times of glycerol (reactant) and water (solvent), which can be used as probe parameters for the strength of the liquid/surface interaction inferred by the  $T_1/T_2$  ratio,<sup>29,30,35,41,42</sup> together with STEM analysis to probe surface morphology and how this links with catalyst activity and adsorption properties. Unlike single values of  $T_1$  and  $T_2$ , the ratio  $T_1/T_2$  represents a much more robust measurement, as this is independent of pore geometry and size; hence, it allows a more direct comparison between different materials.<sup>35,43</sup> Previous studies with NMR relaxation methods on oxidation

of polyols in aqueous and methanol solutions over Au/TiO<sub>2</sub> catalysts have shown that the adsorption properties of these molecules over the catalyst surface have a strong effect on conversion. Adsorption properties were strongly influenced by the type of solvent and the structure of the diol.<sup>16,17</sup>

In this work, we are interested in how competitive adsorption over the catalyst surface affects the reaction pattern and glycerol conversion. In doing this, we also demonstrate the effect of the surface morphology of the catalyst on the NMR relaxation times of adsorbed species, an aspect that has been largely unexplored. Typical two-dimensional  $T_1$ - $T_2$  plots of glycerol and water inside different solid samples are shown in Figure 3.

In all cases, a single peak is observed, with glycerol giving rise to broader peaks due to the greater uncertainty involved in fitting the exponential decay function for short  $T_2$  relaxation

times.<sup>53</sup> Similar plots have been observed when studying adsorption of water and hydrocarbons on Ag/Al<sub>2</sub>O<sub>3</sub> catalysts.<sup>41</sup> It is noted that the shape of the peaks is determined predominantly by the raw data quality (degree of smoothing on inversion<sup>44</sup>) and is not considered representative of physical sample properties. The position of the dashed diagonal in each plot is determined from the maximum peak intensity and corresponds to the  $T_1/T_2$  ratio. This ratio is considered to be an indicator of the strength of interaction between the liquid and the solid surface. An increase in the magnitude of  $T_1/T_2$  indicates an increase in the strength of the surface interaction of a given molecular species with the surface.<sup>30,35</sup> The  $T_1/T_2$  numerical values for glycerol and water over the Au/TiO<sub>2</sub> catalyst as a function of the Au mean particle size (and the corresponding metal loading) are reported in Figure 4.

It is noted that the  $T_1/T_2$  values recorded for the 0% Au/TiO<sub>2</sub> sample (not shown on the plot) are the lowest, with values of  $T_1/T_2 = 60$  for glycerol and  $T_1/T_2 = 12$  for water. The deposition of gold nanoparticles increases the  $T_1/T_2$  for both glycerol and water; however, there are major differences between the two molecules. From Figure 4 it can be observed that the  $T_1/T_2$  of water increases steeply at low Au content and reaches a plateau at higher metal loading. This suggests that the increase in Au loading has the effect of increasing the strength of interaction of water with the catalyst surface. In the case of glycerol, the metal deposition at low Au loading also produces a significant increase in  $T_1/T_2$ , which increases from  $T_1/T_2 = 60$  for 0% Au/TiO<sub>2</sub> up to  $T_1/T_2 = 109$  for 0.5% Au/TiO<sub>2</sub>. However, it can be clearly seen that the  $T_1/T_2$  ratio of glycerol starts dropping with increasing Au loading, and for the 5% Au/TiO<sub>2</sub> catalyst, water becomes dominant over the surface with a  $T_1/T_2$  higher relative to glycerol. Such a very dramatic change, compared to the 0.5% Au/TiO<sub>2</sub> catalyst, indicates that the Au loading, and corresponding Au particle size, is significantly affecting the adsorption properties of these two species.

It is interesting to note that the significant decrease in  $T_1/T_2$  for glycerol relative to water, when moving from the 0.5% to the 1.5% Au/TiO<sub>2</sub> sample, corresponds to a significant drop in conversion observed for the 1.5% Au/TiO<sub>2</sub> sample compared to the 0.5% Au/TiO<sub>2</sub> sample. By comparing the  $T_1/T_2$  adsorption data for the 0.5, 1.5, 3, and 5% Au/TiO<sub>2</sub> samples with the reaction data, it is clear that the increase in metal loading results in a reduced adsorption interaction of glycerol with the catalyst, which corresponds with the reduced activity of the catalyst. This strongly suggests that the affinity of the catalyst surface toward glycerol and water is crucial in determining the catalytic activity. In particular, a stronger affinity of the Au/TiO<sub>2</sub> surface for glycerol relative to water

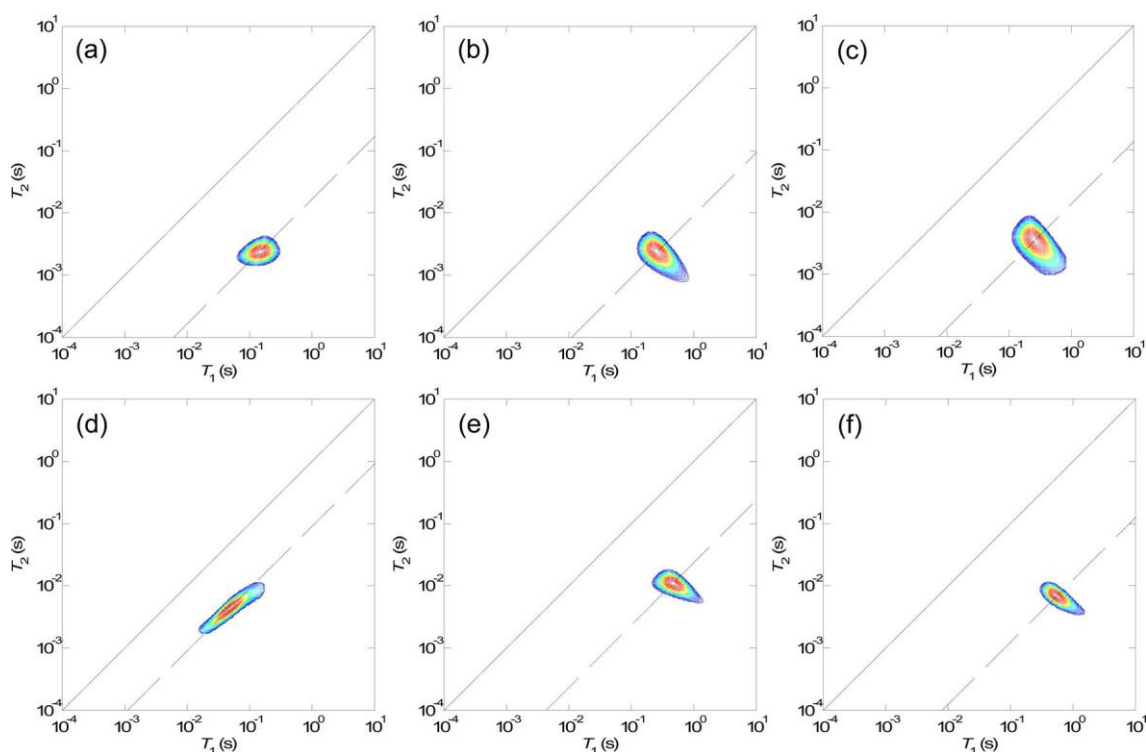


Figure 3.  $T_1$ - $T_2$  plots for: (a) glycerol in 0% Au/TiO<sub>2</sub>; (b) glycerol in 0.5% Au/TiO<sub>2</sub>; (c) glycerol in 5% Au/TiO<sub>2</sub>; (d) water in 0% Au/TiO<sub>2</sub>; (e) water in 0.5% Au/TiO<sub>2</sub>; (f) water in 5% Au/TiO<sub>2</sub>. The solid diagonal line indicates  $T_1/T_2 = 1$ . The dotted diagonal line indicates the  $T_1/T_2$  of the liquid over the catalyst surface.

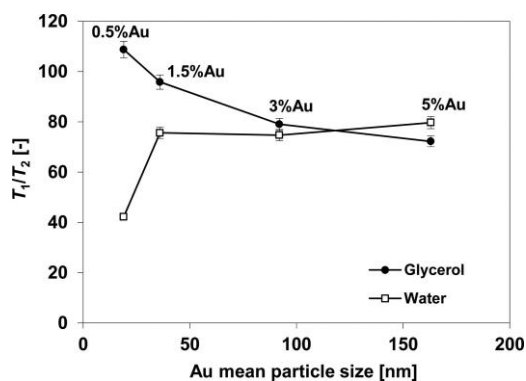


Figure 4.  $T_1/T_2$  ratio for glycerol and water over Au/TiO<sub>2</sub> catalysts as a function of Au mean particle size. Indication of the corresponding Au loading is also reported. The solid line is a guide to the eye.

leads to a much greater reactivity compared to the case where the relative affinity of glycerol decreases; that is, water becomes the dominant species over the surface. We have previously shown that the strength of adsorption of diols in Au/TiO<sub>2</sub> catalysts is affected by the type of solvent and can be related to its reactivity.<sup>16,17</sup> The results reported here support such earlier findings.

**Effect of Au Particle Size on Activity and Molecular Adsorption of Glycerol.** As shown in Figure 4, the competitive adsorption effect observed in this work is clearly related to the Au loading. While for water the  $T_1/T_2$  trend finds a plausible explanation in terms of increasing Au content, the  $T_1/T_2$  trend observed for glycerol is more puzzling, as it shows a spike at low Au loading and it then drops at higher loading. To further investigate this aspect, in addition to NMR relaxation measurements, we have carried out STEM analysis

of the catalysts at different metal loadings to understand if and how the morphology of the surface is affected by the different Au loadings, and how this is related to the reactivity profile and importantly to the adsorption profile obtained by NMR relaxation measurements.

Figure 5 shows typical STEM images of the catalysts at different metal loadings. In this imaging mode, heavier elements appear brighter; the brightest particles are gold aggregates. The straight features in some corners are the metal bars supporting the sample for STEM analysis. The TiO<sub>2</sub> particles have a similar structure in all the samples, with a size in the 10–25 nm range, as expected for P25 titanium dioxide. The particle size distribution (PSD) of Au particles, normalized over the total count, is shown in Figure 6.

The 0.5% Au/TiO<sub>2</sub> sample presents well dispersed Au particles, with a rather narrow PSD, with a well-defined peak at ~10 nm. The mean particle size is 19 nm, with a median value of 12 nm and a standard deviation of 21 nm. As the Au loading increases, the typical dimension of the particles starts increasing. For the 1.5% Au/TiO<sub>2</sub> sample, we observe the peak of the distribution at ~20 nm, a mean particle size of 36 nm, with a median value of 25 nm and a standard deviation of 50 nm, with particle diameter up to 190 nm. For Au loadings of 3 and 5%, small (<50 nm) particles become less common, particularly for the 5% sample, and the vast majority of the gold is aggregated in much larger particles, as can be observed by inspection of Figure 5 and Figure 6. The PSD for the 3% Au/TiO<sub>2</sub> sample has a peak in the range 40–50 nm, with a mean diameter of 92 nm, a median value of 45 nm, and a standard deviation of 106 nm. The 5% Au/TiO<sub>2</sub> sample shows the presence of fewer but significantly larger gold particles, most of them with a size in the range 50–200 nm, with a mean diameter of 163 nm, median value of 96 nm, and a very broad

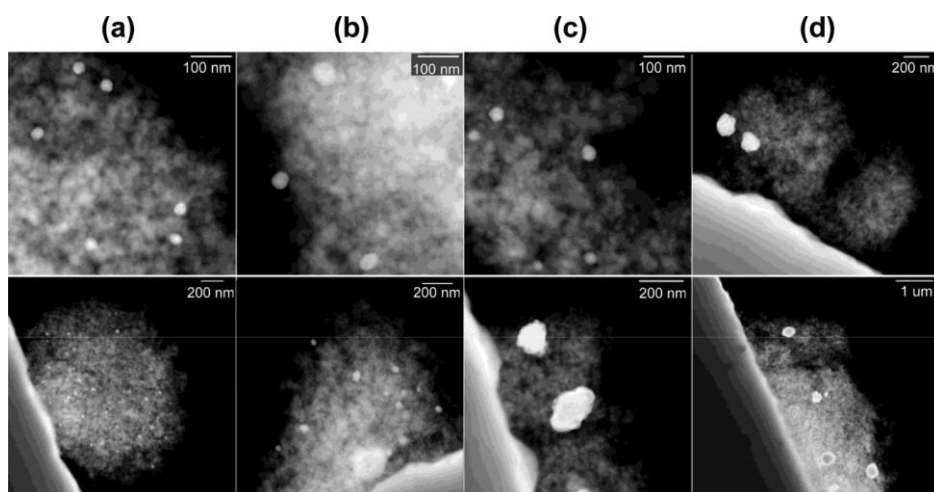


Figure 5. Typical STEM dark field images of the catalyst for (a) 0.5%, (b) 1.5%, (c) 3%, and (d) 5% Au loadings. Gold is brighter than TiO<sub>2</sub>; the straight surfaces appearing in some corners are the support grid for the STEM specimen. At higher loadings, large aggregates (>100 nm) contain most of the gold.

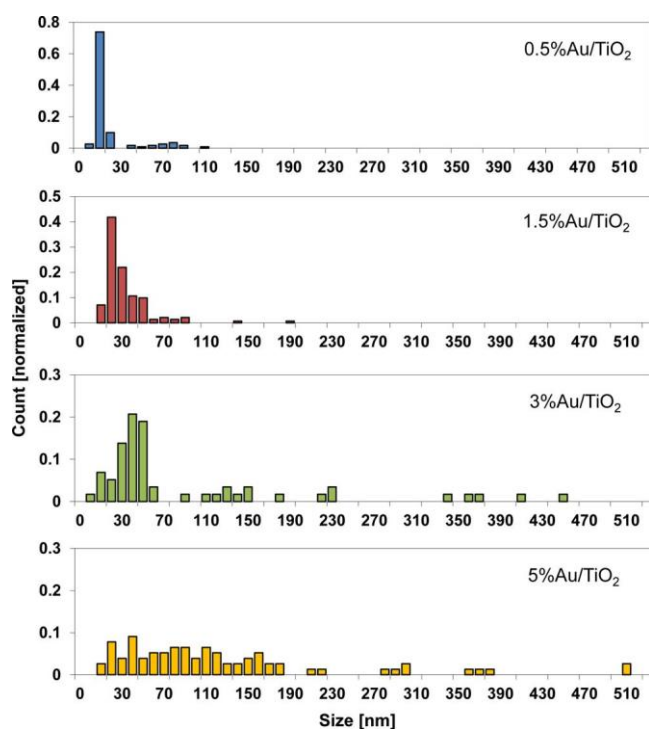


Figure 6. Size distribution of the Au particles over TiO<sub>2</sub> for different Au loadings.

distribution with a standard deviation of 246 nm. The total count for all samples was of over a hundred particles and comparable in all cases. It is clear that as the gold loading is increasing, the PSD becomes broader, shifting toward larger particles. It has previously been reported that low Au loading favors the formation of smaller, better dispersed particles,<sup>45</sup> which is in agreement with our observations. This might be due to a reduced “clustering” effect during the catalyst preparation process.

Glycerol oxidation reactions are very sensitive to Au particle size. Dimitratos et al.<sup>24</sup> have studied glycerol oxidation over Au/C catalysts and reported that above a gold particle size of 10 nm the catalytic activity experiences a dramatic drop. Ketchie et al.<sup>46</sup> have reported analogous findings, showing a

significant drop in catalyst activity when moving from 12 to 20 nm gold particles. Our current findings strongly support this correlation between catalyst activity and Au particle size. Indeed, the results reported here show that the 0.5% Au/TiO<sub>2</sub> sample is the catalyst with the highest activity and has a narrow Au PSD highly centered around 10 nm. As shown in Figure 2, the catalyst activity drops significantly for the 1.5% Au/TiO<sub>2</sub> sample, which has an Au PSD centered on 20 nm. This agrees very well with the earlier experimental reports discussed above and also with previously reported computational studies relating particle size and catalyst activity.<sup>38,39</sup> Another effect which may be in operation is the irreversible binding of reaction products, i.e. product inhibition. It has been shown that the products of glycerol oxidation can poison the catalyst by blocking active sites.<sup>14</sup> Two of the major products in this study, glycolic acid and formic acid, do not have a strong affinity for catalyst binding; however, the third major product, glyceric acid, does bind strongly to gold catalyst surface. On the basis of the study by Zope and Davis,<sup>14</sup> we conclude that it is highly unlikely that the small amounts of glyceric acid formed in this study would account for the marked decrease in activity observed with increasing weight loading.

It is now of interest to analyze the NMR relaxation results in light of the Au PSD obtained by STEM. Here, it is important to note that the T<sub>1</sub>/T<sub>2</sub> ratio probes an “average” interaction strength of the species adsorbed within the catalyst with the overall catalyst surface, that is, Au + TiO<sub>2</sub>, and not the specific interaction with Au particles. However, given that the TiO<sub>2</sub> support is the same in all cases, it is reasonable to assume that the distribution of Au particles will be mostly responsible for any changes in T<sub>1</sub>/T<sub>2</sub>. The STEM results suggest that, unlike water, the strength of interaction of glycerol is highly affected by the size of the gold particles over the TiO<sub>2</sub> surface. In particular, a low Au loading favors the deposition of smaller gold particles; for such samples, a higher T<sub>1</sub>/T<sub>2</sub> of glycerol is observed relative to higher Au loading samples, with the latter showing much larger gold particles. The increase of the T<sub>1</sub>/T<sub>2</sub> ratio of glycerol with decreasing Au loading, hence decreasing particle size, strongly suggests that smaller Au particles are much stronger relaxation sinks for glycerol, which can be related to their higher adsorption strength. In particular, we observe that catalysts with a PSD shifted toward smaller gold



particles show a higher affinity for glycerol, as measured by its  $T_1/T_2$  ratio. This may play an important role in the promoting effect of smaller gold particles in enhancing catalyst activity for glycerol oxidation, which has been documented in the literature. This result is of significance because it gives the first experimental evidence that smaller gold particles have higher affinity toward glycerol. This has significant implications in understanding gold catalysis of polyols and is in agreement with computational and theoretical studies previously reported.<sup>38,39</sup> With regard to the role that the oxygen plays in the reaction, it has been demonstrated by DFT studies and labeling experiments that the oxygen incorporated into the substrate originates from hydroxyl species, not dissociated molecular oxygen.<sup>47</sup> The molecular oxygen replenished the hydroxyl species via the formation and destruction of peroxide species. It has been shown previously that large particles (>20 nm) decompose peroxides more slowly than smaller particles;<sup>48</sup> this phenomenon may contribute to the results reported in this study.

## CONCLUSIONS

The effect of gold loading and particle size on the oxidation of glycerol in aqueous solutions has been investigated using catalytic reaction studies, NMR relaxation methods, and STEM microscopy analysis. The results suggest that a low gold loading has several important implications in affecting catalyst activity, as it results in a better dispersion of smaller gold nanoparticles over the  $TiO_2$  support. NMR relaxation studies reveal that smaller gold particles improve the overall condition for the glycerol adsorption over the surface, as measured by the  $T_1/T_2$  ratio. This suggests that smaller Au particles act as much stronger adsorption sites for glycerol, suggesting that the gold particle size distribution is a very important parameter to consider in order to improve the conditions for a better glycerol adsorption over the surface. The results reveal insights into molecular adsorption on gold catalysts and contribute to advancing the understanding of gold catalysis of biorenewable feedstocks, such as glycerol.

## AUTHOR INFORMATION

Corresponding Author

\*E-mail: [cd419@cam.ac.uk](mailto:cd419@cam.ac.uk). Tel: 01223-334796.

ORCID 

Carmine D'Agostino: 0000-0003-3391-8320

Notes

The authors declare no competing financial interest.

## ACKNOWLEDGMENTS

Carmine D'Agostino would like to acknowledge Wolfson College, Cambridge, for supporting his research activities. We also wish to thank the EPSRC and the CASTech consortium for supporting this work (EP/G011397/1). Caterina Ducati and Giorgio Divitini acknowledge funding from ERC grant number 259619 PHOTO EM and from the European Union Seventh Framework Programme under Grant Agreement 312483 - ESTEEM2.

## REFERENCES

- (1) Dimitratos, N.; Lopez-Sanchez, J. A.; Meenakshisundaram, S.; Anthonykutti, J. M.; Brett, G.; Carley, A. F.; Taylor, S. H.; Knight, D. W.; Hutchings, G. J. *Green Chem.* 2009, 11, 1209–1216.
- (2) Taarning, E.; Nielsen, I. S.; Egeblad, K.; Madsen, R.; Christensen, C. H. *ChemSusChem* 2008, 1, 75–78.
- (3) Demirel, S.; Lehnert, K.; Lucas, M.; Claus, P. *Appl. Catal., B* 2007, 70, 637–643.
- (4) Taarning, E.; Madsen, A. T.; Marchetti, J. M.; Egeblad, K.; Christensen, C. H. *Green Chem.* 2008, 10, 408–414.
- (5) Pagliaro, M.; Ciriminna, R.; Kimura, H.; Rossi, M.; Della Pina, C. *Angew. Chem., Int. Ed.* 2007, 46, 4434–4440.
- (6) Prati, L.; Porta, F. *Appl. Catal., A* 2005, 291, 199–203.
- (7) Corma, A.; Huber, G. W.; Sauvanauda, L.; O'Connor, P. J. *Catal.* 2008, 257, 163–171.
- (8) Abbott, A. P.; Cullis, P. M.; Gibson, M. J.; Harris, R. C.; Raven, E. *Green Chem.* 2007, 9, 868–872.
- (9) Abbott, A. P.; Harris, R. C.; Ryder, K. S.; D'Agostino, C.; Gladden, L. F.; Mantle, M. D. *Green Chem.* 2011, 13, 82–90.
- (10) Carrettin, S.; McMorn, P.; Johnston, P.; Griffin, K.; Hutchings, G. J. *Chem. Commun.* 2002, 696–697.
- (11) Bianchi, C. L.; Canton, P.; Dimitratos, N.; Porta, F.; Prati, L. *Catal. Today* 2005, 102, 203–212.
- (12) Kondrat, S. A.; Miedziak, P. J.; Douthwaite, M.; Brett, G. L.; Davies, T. E.; Morgan, D. J.; Edwards, J. K.; Knight, D. W.; Kiely, C. J.; Taylor, S. H.; Hutchings, G. J. *ChemSusChem* 2014, 7, 1326–1334.
- (13) Demirel-Gulen, S.; Lucas, M.; Claus, P. *Catal. Today* 2005, 102, 166–172.
- (14) Zope, B. N.; Davis, R. J. *Green Chem.* 2011, 13, 3484–3491.
- (15) Bianchi, C.; Porta, F.; Prati, L.; Rossi, M. *Top. Catal.* 2000, 13, 231–236.
- (16) D'Agostino, C.; Brett, G. L.; Miedziak, P. J.; Knight, D. W.; Hutchings, G. J.; Gladden, L. F.; Mantle, M. D. *Chem. - Eur. J.* 2012, 18 (45), 14426–14433.
- (17) D'Agostino, C.; Kotionova, T.; Mitchell, J.; Miedziak, P. J.; Knight, D. W.; Taylor, S. H.; Hutchings, G. J.; Gladden, L. F.; Mantle, M. D. *Chem. - Eur. J.* 2013, 19, 11725–11732.
- (18) Prati, L.; Rossi, M. *J. Catal.* 1998, 176, 552–560.
- (19) Comotti, M.; Della Pina, C.; Matarrese, R.; Rossi, M.; Siani, A. *Appl. Catal., A* 2005, 291, 204–209.
- (20) Hutchings, G. J.; Haruta, M. *Appl. Catal., A* 2005, 291, 2–5.
- (21) Mertens, P. G. N.; Vankelecom, I. F. J.; Jacobs, P. A.; De Vos, D. E. *Gold Bull.* 2005, 38, 157–162.
- (22) Hayashi, T.; Inagaki, T.; Itayama, N.; Baba, H. *Catal. Today* 2006, 117, 210–213.
- (23) Mantle, M. D.; Enache, D. I.; Nowicka, E.; Davies, S. P.; Edwards, J. K.; D'Agostino, C.; Mascarenhas, D. P.; Durham, L.; Sankar, M.; Knight, D. W.; Gladden, L. F.; Taylor, S. H.; Hutchings, G. J. *J. Phys. Chem. C* 2011, 115, 1073–1079.
- (24) Dimitratos, N.; Lopez-Sanchez, J. A.; Lennon, D.; Porta, F.; Prati, L.; Villa, A. *Catal. Lett.* 2006, 108, 147–153.
- (25) D'Agostino, C.; Ryabenkova, Y.; Miedziak, P. J.; Taylor, S. H.; Hutchings, G. J.; Gladden, L. F.; Mantle, M. D. *Catal. Sci. Technol.* 2014, 4, 1313–1322.
- (26) Mallat, T.; Baiker, A. *Chem. Rev.* 2004, 104, 3037–3058.
- (27) Villa, A.; Veith, G. M.; Prati, L. *Angew. Chem., Int. Ed.* 2010, 49, 4499–4502.
- (28) Xu, J.; Zhang, H.; Zhao, Y.; Yu, B.; Chen, S.; Li, Y.; Hao, L.; Liu, Z. *Green Chem.* 2013, 15, 1520–1525.
- (29) Mitchell, J.; Broche, L. M.; Chandrasekera, T. C.; Lurie, D. J.; Gladden, L. F. *J. Phys. Chem. C* 2013, 117, 17699–17706.
- (30) Weber, D.; Mitchell, J.; McGregor, J.; Gladden, L. F. *J. Phys. Chem. C* 2009, 113, 6610–6615.
- (31) McDonald, P. J.; Korb, J. P.; Mitchell, J.; Montellhet, L. *Phys. Rev. E* 2005, 72, 9.
- (32) McDonald, P. J.; Mitchell, J.; Mulheron, M.; Aptaker, P. S.; Korb, J. P.; Montellhet, L. *Cem. Concr. Res.* 2007, 37, 303–309.
- (33) Korb, J. P. *New J. Phys.* 2011, 13, 26.
- (34) Godefroy, S.; Fleury, M.; Deflandre, F.; Korb, J. P. *J. Phys. Chem. B* 2002, 106, 11183–11190.
- (35) D'Agostino, C.; Mitchell, J.; Mantle, M. D.; Gladden, L. F. *Chem. - Eur. J.* 2014, 20, 13009–13015.

- (36) Murdoch, M.; Waterhouse, G. I. N.; Nadeem, M. A.; Metson, J. B.; Keane, M. A.; Howe, R. F.; Llorca, J.; Idriss, H. *Nat. Chem.* 2011, 3, 489–492.
- (37) Zane, F.; Trevisan, V.; Pinna, F.; Signoreto, M.; Menegazzo, F. *Appl. Catal., B* 2009, 89, 303–308.
- (38) van Santen, R. A.; Neurock, M. *Molecular heterogeneous catalysis: A conceptual and computational approach*; Wiley-VCH: Weinheim, Germany, 2006.
- (39) Ntho, T.; Aluha, J.; Gqogqa, P.; Raphulu, M.; Patrick, G. *React. Kinet., Mech. Catal.* 2013, 109, 133–148.
- (40) D'Agostino, C.; Feaviour, M. R.; Brett, G. L.; Mitchell, J.; York, A. P. E.; Hutchings, G. J.; Mantle, M. D.; Gladden, L. F. *Catal. Sci. Technol.* 2016, 6, 7896.
- (41) Ralphs, K.; D'Agostino, C.; Burch, R.; Chansai, S.; Gladden, L. F.; Hardacre, C.; James, S. L.; Mitchell, J.; Taylor, S. *F. R. Catal. Sci. Technol.* 2014, 4, 531–539.
- (42) Gladden, L. F.; Mitchell, J. *New J. Phys.* 2011, 13, 46.
- (43) D'Agostino, C.; Feaviour, M. R.; Brett, G. L.; Mitchell, J.; York, A. P. E.; Hutchings, G. J.; Mantle, M. D.; Gladden, L. F. *Catal. Sci. Technol.* 2016, 6, 7896–7901.
- (44) Mitchell, J.; Chandrasekera, T. C.; Gladden, L. F. *Prog. Nucl. Magn. Reson. Spectrosc.* 2012, 62, 34–50.
- (45) Xin, J.-Y.; Lin, K.; Wang, Y.; Xia, C.-G. *Int. J. Mol. Sci.* 2014, 15, 21603–21620.
- (46) Ketchie, W. C.; Fang, Y.-L.; Wong, M. S.; Murayama, M.; Davis, R. J. *J. Catal.* 2007, 250, 94–101.
- (47) Zope, B. N.; Hibbitts, D. D.; Neurock, M.; Davis, R. J. *Science* 2010, 330, 74.
- (48) Ketchie, W. C.; Murayama, M.; Davis, R. J. *Top. Catal.* 2007, 44, 307–317.